ULTRA SONO GRAPHY

# Nerve entrapment syndromes: detection by ultrasound

Christoph Schwabl[1], Gernot Schmidle[2], Peter Kaiser[2], Elena Drakonaki[3], Mihra S. Taljanovic[4], Andrea S. Klauser[1]

[1]Radiology Department, Medical University Innsbruck, Innsbruck, Austria; [2]Department for Orthopedics and Traumatology, Medical University Innsbruck, Innsbruck, Austria; [3]Independent MSK Radiology Practice, Heraklion, Greece; [4]Department of Medical Imaging, Banner University Medical Center, The University of Arizona, College of Medicine, Tucson, AZ, USA

REVIEW ARTICLE

https://doi.org/10.14366/usg.22186
eISSN: 2288-5943
Ultrasonography 2023;42:376-387

Nerve entrapment syndromes are commonly encountered in clinical practice. Accurate diagnosis and management require a knowledge of peripheral neuroanatomy and the recognition of key clinical symptoms and findings. Nerve entrapment syndromes are frequently associated with structural abnormalities of the affected nerve. Therefore, imaging allows the evaluation of the cause, severity, and etiology of the entrapment. High-resolution ultrasonography can depict early and chronic morphological changes within the entire nerve course and is therefore an ideal modality for diagnosing various nerve entrapment syndromes in different regions. This review article presents some of the most common types of nerve entrapment, with special focus on ultrasound imaging and key findings.

Keywords: Entrapment neuropathy; Median nerve; Carpal tunnel syndrome; Ultrasonography; Ulnar nerve

Key points: High-resolution ultrasonography is a feasible, fast, and reliable method to diagnose nerve entrapment syndromes. Ultrasound findings include enlargement of the nerve at the site of compression, hourglass narrowing, loss of the echotexture, and echogenic perineural fibrosis. Anatomical landmarks and morphological features are key for understanding and identifying nerve entrapments on ultrasonography.

Received: November 11, 2022
Revised: January 17, 2023
Accepted: February 2, 2023

Correspondence to:
Christoph Schwabl, MD, Radiology Department, Medical University Innsbruck, Anichstrasse 35, A-6020 Innsbruck, Austria

Tel. +4351250483950
Fax. +4351250422758
E-mail: Christoph.schwabl@i-med.ac.at



How to cite this article:
Schwabl C, Schmidle G, Kaiser P, Drakonaki E, Taljanovic MS, Klauser AS. Nerve entrapment syndromes: detection by ultrasound. Ultrasonography. 2023 Jul;42(3):376-387.

## Introduction

Nerve entrapment syndromes are frequently associated with structural abnormalities, such as compression and displacement [1]. They generally have a typical clinical presentation, which may begin with paresthesia and distal numbness and often progresses over time to muscle weakness and muscle wasting, depending on the extent of axonal damage at later stages [2]. In addition to patients' clinical presentation, imaging modalities are increasingly being used to accurately assess nerve entrapments.

Magnetic resonance imaging (MRI) is useful for dedicated nerve entrapment assessment in a focal region, especially where ultrasonography (US) has limited access, but in most cases, US is an

appropriate method to provide an overview of the entire length of the nerve. The progressive refinement of broadband transducers with high frequencies and improved near-field resolution has enhanced the potential of US to evaluate a variety of nerve entrapment syndromes [3]. US can define the level of nerve entrapment, at which MRI can then generate an overview to exclude possible secondary causes of entrapment, such as articular ganglia. Electromyography allows the assessment of nerve function, but does not precisely determine the type and degree of change.

Measuring the nerve's cross-sectional area (CSA) is one of the most important tools in the diagnosis of nerve entrapment syndromes. However, a defined CSA value for each peripheral nerve is still missing and a frequent point of discussion because it may differ in patients according to age, sex, physical habitus, comorbidities such as type 2 diabetes mellitus, or the imaging modality used (e.g., MRI or US) [4–7]. Furthermore, frequent work with one's hands or fingers, such as among professional musicians, seems to lead to greater CSAs (e.g., in the median nerve) [8].

This article will focus on the diagnosis of the most common nerve entrapment syndromes via US, with particular attention paid to imaging landmarks and morphological features.

## Pathophysiology and Sonographic Morphology of Nerve Compression

The main mechanism of nerve injury in compression is degradation and thinning of the myelin sheath due to compressive forces resulting in microvascular damage, while the morphology and neuromuscular junctions remain intact [9,10]. Mild degrees of compression may obstruct venous flow, causing congestion and edema, while more severe and consistent compression results in arterial ischemia. Prolonged or repetitive compression results in inflammation, fibrosis, and demyelination. Loss of myelination leads to disruptions in the speed of axonal signaling, and at its most severe can result in a partial or complete block of action potentials through the affected nerve segment. With persistent compression, the combination of these factors may lead to axonal degeneration. This portends a poorer prognosis and more prolonged recovery; remyelination may take a matter of weeks, while axonal regrowth is glacially slow, at approximately 1 mm/day [11,12].

These changes in the nerve lead to typical appearances on US. A normal nerve has a typical honeycomb-like appearance with hypoechoic nerve fascicles and hyperechoic interfascicular perineurium [13]. With entrapment, this appearance on US changes to an irregular and blurred appearance with echogenic perineural fibrosis and the loss of fascicular echotexture [14]. Initially, the nerve often appears hypoechoic and swollen, which can change over time in chronic entrapment to intraneural fibrotic changes with echogenic spots and, therefore, a more echogenic appearance of the nerve, finally leading to the presentation of a smaller CSA due to edema regression (Fig. 1).

Nerve swelling can be measured by the CSA, which is increased

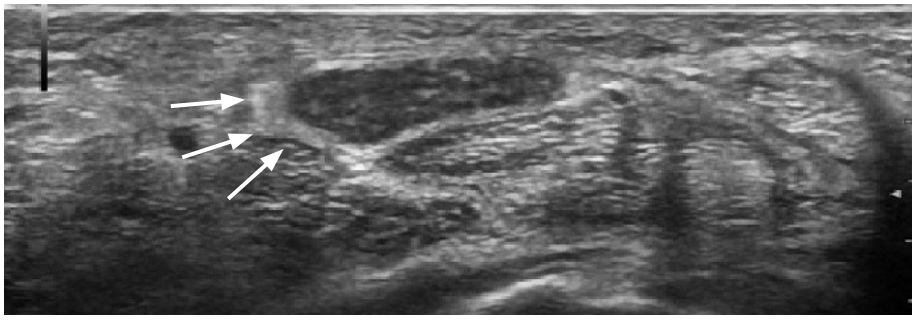

A

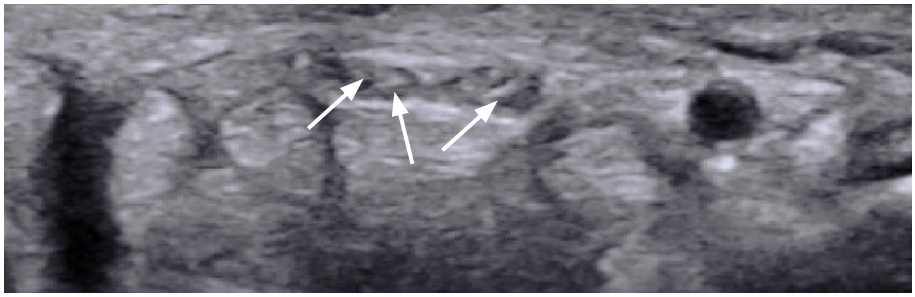

B

Fig. 1. A 78-year-old patient with unilateral symptoms of carpal tunnel syndrome.
A. The ultrasonography examination reveals a swollen, hypoechoic nerve with a thickened perineurium on the affected side (arrows). B. The other hand shows a normal median nerve inside the carpal tunnel with a typical honeycomb-like appearance, with hypoechoic nerve fascicles and hyperechoic interfascicular perineurium (arrows).

in cases of focal compression and entrapment. Therefore, a measurement proximal to the entrapment level and a measurement at the maximal CSA at the compression site is recommended. This procedure enables the calculation of delta (i.e., difference) values, which allows an objective gradation of nerve thickening in nerve entrapment by US [15,16].

## Median Nerve

Carpal tunnel syndrome (CTS) is the most common entrapment neuropathy, affecting 9% of women and 0.6% of men, and it is responsible for significant morbidity and occupational absence [17]. It is caused by compression of the median nerve at the wrist as it passes through a space-limited osteofibrous canal. The syndrome is characterized first by intermittent, nocturnal paresthesia and dysesthesia that increase in frequency and occur during waking hours. Subsequently, loss of sensation develops along with weakness and thenar muscle atrophy later in the disease course, which result from extensive axonal degeneration. This sequence of symptoms is quite typical and rarely occurs in disorders other than CTS [18,19].

By allowing direct visualization of the compressed nerve, US provides additional information to that obtained from clinical tests and electrodiagnostic tests and can therefore depict possible causes of secondary CTS and describe anatomical variants, such as a bifid median nerve or a persistent median artery of the forearm, as well as space-occupying lesions, including tenosynovitis and ganglion cysts [20].

As in other nerve entrapment syndromes, US is a suitable method to determine CSA values. Because of the variability of CSA values of the median nerve, it has been proposed to present CSA ratios as a convenient method. A study by Klauser et al. [15] included 643 wrists of 427 patients with a CTS diagnosis based on clinical and nerve conduction studies. CSA measurement of the median nerve was performed at the carpal tunnel level and at the pronator quadratus muscle level. Two parameters were calculated: delta (Δ-CSA), which referred to the difference between proximal and distal measurements, and the ratio (R-CSA), calculated by dividing the distal measurement by the proximal measurement. They found cutoff values for Δ-CSA and R-CSA of 6 $mm^2$ and 1.7, respectively, to distinguish mild from moderate disease, and 9 $mm^2$ and 2.2, respectively, to distinguish moderate from severe disease (Fig. 2).

Besides the constriction of the main nerve, smaller nerve branches can also be affected by entrapment, such as the palmar cutaneous branch, which provides sensation at the thenar eminence. It emerges in a variable location from the proximal aspect towards the transverse carpal ligament and divides into a lateral and a medial portion. The lateral portion supplies the recurrent motor branch for the thenar muscles, whereas the median portion supplies two common volar digital nerves for the index and middle finger [21]. These nerve branches may also be affected in CTS and can be injured during carpal tunnel surgery or entrapped by scarring [22]. US can visualize these small nerve branches, enabling US-guided treatment as well.

If normal CSA values are detected on US, further examination of the median nerve towards the elbow is recommended, at which level entrapment due to hematomas, biceps tendinosis, and bicipitoradial bursitis might be the cause of entrapment.

## Special Forms

The presence of anastomoses may increase the risk of iatrogenic injury during surgical procedures and make it difficult to interpret

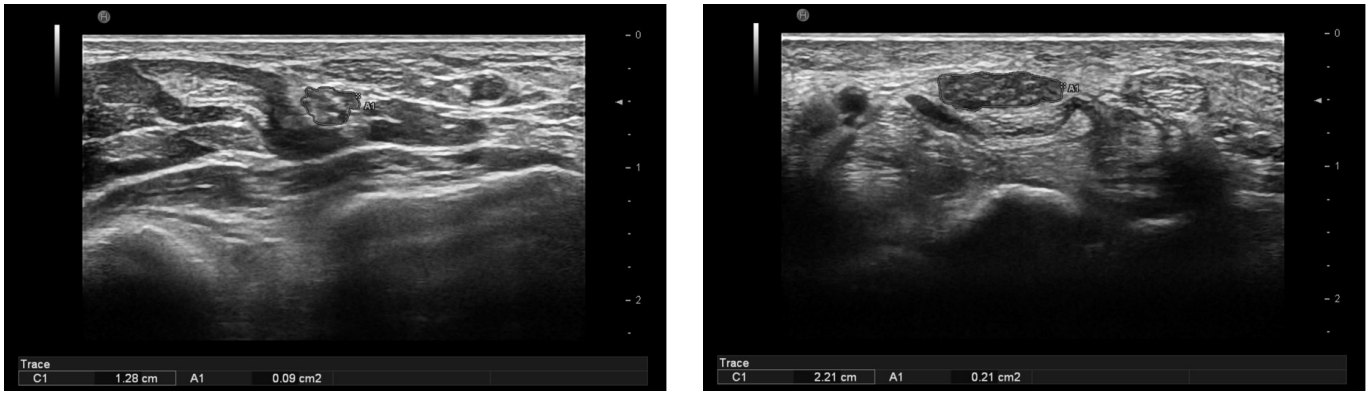


A B

Fig. 2. A 56-year-old patient with the clinical presentation of carpal tunnel syndrome.
On ultrasonography, the cross-sectional area of the median nerve at the level of the pronator quadratus (A) and within the carpal tunnel (B) shows a pathological delta value of 12 $mm^2$. The nerve has a blurred echotexture and is hypoechoic and swollen.

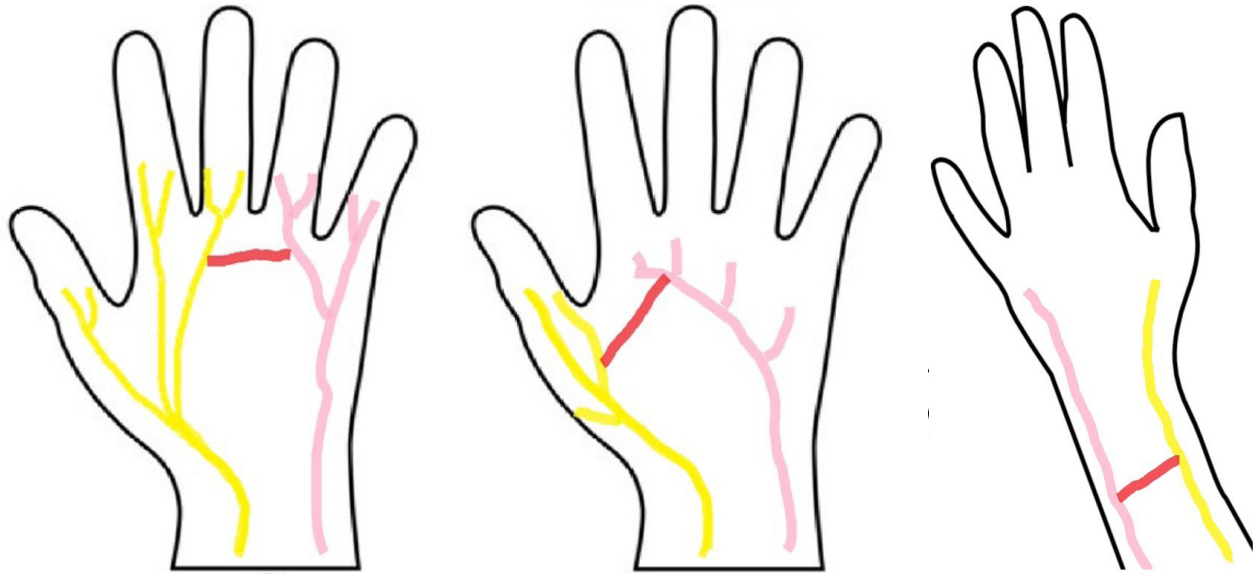


Fig. 3. Schematic diagrams of Berrettini anastomosis (A), Riche-Cannieu anastomosis (B), and Martin-Gruber anastomosis (C).

electrophysiological studies in the diagnosis of neuropathies. These anatomical variations must be differentiated from incomplete nerve lesions, since clinically, variations in the innervation of these small muscles are very important in the sense that, even with a complete lesion of the median or ulnar nerves, some of these muscles may or may not be paralyzed, which may lead to the erroneous conclusion that the nerve is not affected by a complete lesion [23].

Unfortunately, there is not much literature available regarding the clinical implications of these anastomoses. Publications on this would be desirable. Nevertheless, a profound knowledge of these anastomoses is essential for the accurate interpretation of findings and for reducing the risk of iatrogenic injuries during surgical procedures (Fig. 3).

## Martin-Gruber Anastomosis

In a study by Sur et al. [24] the Martin-Gruber anastomosis (MGA) occurred with a prevalence of 15.7%. The MGA emerges as a communicating branch in the cubital fossa from the main trunk of the median nerve, crosses superficial to the flexor digitorum superficialis or flexor digitorum profundus muscles, and then joins the ulnar nerve. The MGA has mainly been reported to supply motor innervation to the thenar, hypothenar, and dorsal interosseous muscles; however, some sensory fibers have also been identified with possibly variable clinical presentations [25,26].

## Riche-Cannieu Anastomosis

The Riche-Cannieu anastomosis (RCA) occurs with a prevalence of 55.5% [25]. The RCA is a palmar anastomosis between the recurrent branch of the median nerve and the deep branch of the ulnar nerve, combining fibers of the ulnar nerve with those of the median nerve, leading to innervation of the thenar muscles [23].

## Berrettini Anastomosis

The Berrettini anastomosis (BA) is an ulnar-to-median sensory nerve connection with a reported prevalence of 61% [25]. With its superficial position and close relation to the flexor retinaculum, usually at the region of the third digit, it is particularly vulnerable to iatrogenic injuries. While the BA is usually clinically silent, it may be associated with atypical patterns of sensory innervation, leading to a complex neurological assessment and unexpected patterns of sensory disturbance [27,28].

## Ulnar Nerve

Ulnar neuropathy, often occurring at the elbow, is the second most common mononeuropathy seen in outpatient neurology settings [29]. Throughout its course, compression might occur in several locations; therefore, the nerve must be scanned over its entire course. Proximal compression might occur at the arcade of Struthers, a fibrous band running from the medial head of the triceps to the medial intermuscular septum, before the nerve passes through the

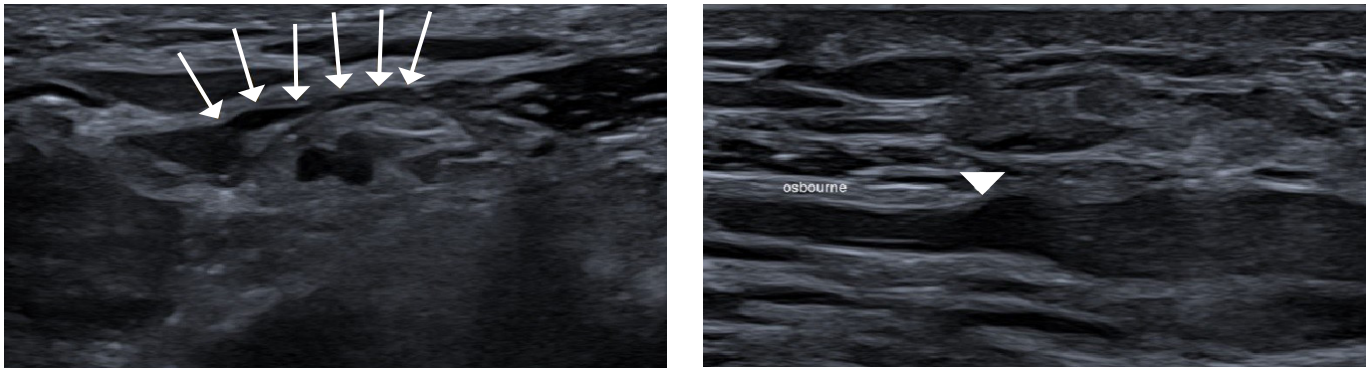


A B

Fig. 4. A 36-year-old patient presenting with pain and numbness at the ulnar forearm, starting from the elbow.
A, B. Ultrasonography shows a thick hypoechoic Osborne ligament (A, arrows) with a swollen ulnar nerve proximal to the strangulation point (B, arrowhead).

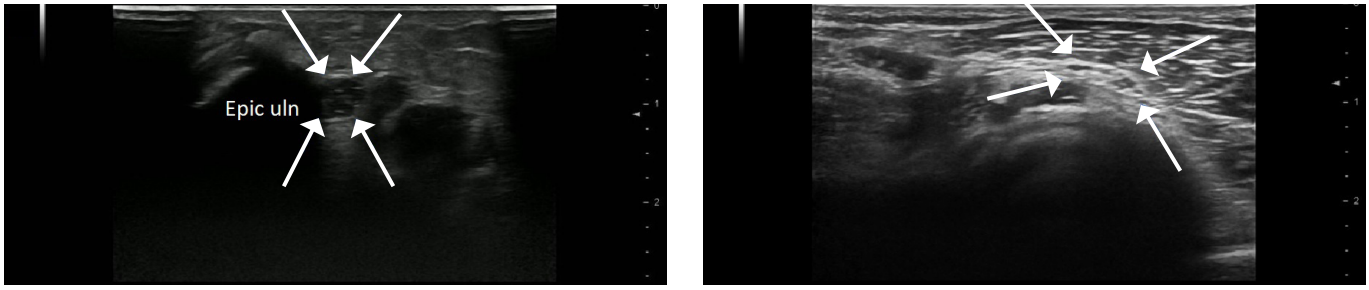


A B

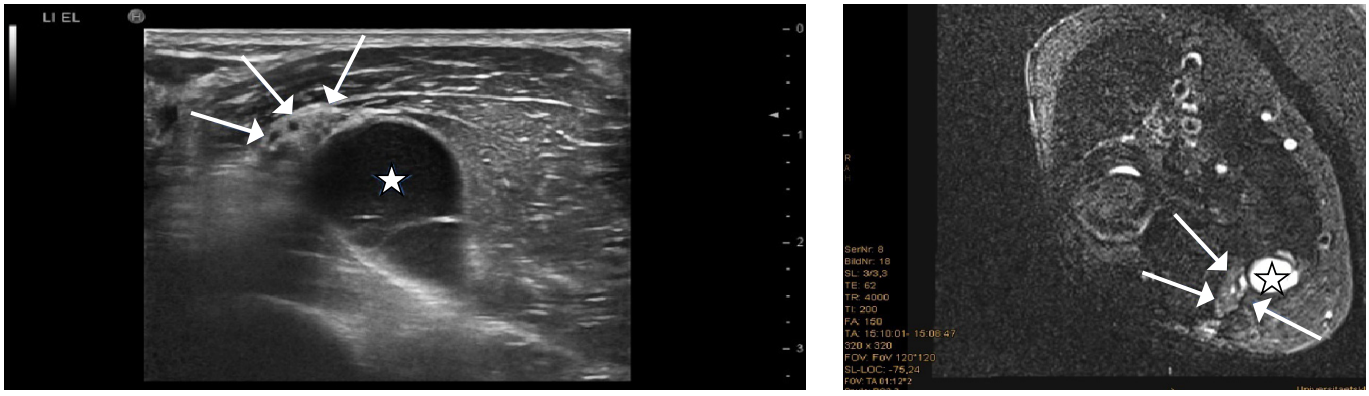


C D

Fig. 5. A 53-year-old patient presenting with persistent cubital tunnel syndrome.
A, B. Ultrasonography examination shows a hypoechoic, swollen ulnar nerve, within the cubital tunnel (A) with echogenic perineurium (B) (arrows). C. A large septated joint ganglion (star) with displacement of the nerve (arrows) in the cubital tunnel can be visualized adjacent to the nerve. D. T2-weighted axial magnetic resonance imaging with fat saturation shows the ganglion (star) and the swollen hyperintense nerve (arrows) with a better overview of the region.

epicondylar (ulnar) groove, located between the medial epicondyle and the olecranon. An anomalous anconeus epitrochlearis muscle overlying the ulnar nerve and extending between the olecranon and medial epicondyle may sometimes be a source of compression in this region. The cubital tunnel is located just distal to the elbow joint, and it is defined by the medial collateral ligament and the thickened fascia known as the Osborne (arcuate) ligament. This ligament lies between the medial and ulnar heads of the flexor carpi

ulnaris and can also lead to entrapment of the nerve (Fig. 4).

The normal ulnar nerve CSA at the elbow is 8 $mm^2$ to 11 $mm^2$, with larger values suggesting focal compression (Fig. 5A) [30]. However, the diagnosis of cubital tunnel syndrome is not only based on the CSA but also on textural analysis of the nerve, and a thickened and hyperechoic epineurium might be one of the earlier changes, before an increased cubital-to-humeral nerve area ratio occurs (Fig. 5B) [31,32].

Ganglia arising from the elbow joint can also lead to cubital tunnel syndrome (Fig. 5C, D). Distal compression might occur within the Guyon canal. In Guyon canal syndrome, the ulnar nerve is compressed, leading to paresthesia and later complaints of motor abnormalities in the distribution of the fourth and fifth digits, as well as weakness in the midpalmar muscles. Guyon canal syndrome most commonly results from compression of the nerve within the canal by a space-occupying lesion, such as a mass, varix, ulnar artery pseudoaneurysm, or ganglion cyst or extrinsic compression, such as by handlebars in avid bicyclists or in players of golf and racquet sports [33–36].

US has emerged as a reliable method for assessing ulnar neuropathy.

## Radial Nerve

The annual incidence of this peripheral compressive neuropathy is approximately 0.03% as compared with CTS, which ranges between 0.1% and 0.35% [37,38]. Radial tunnel syndrome is an uncommon condition caused by entrapment of the radial or posterior interosseous nerve [39,40]. It presents primarily as pain within the mobile wad, approximately 3–5 cm distal to the lateral epicondyle, for which reason lateral epicondylitis is a major possibility considered in the differential diagnosis. Various compressive etiologies have been described, including fascial bands, radial recurrent vessels, the proximal edge of the supinator, and various space-occupying lesions (ganglions, hemangioma, lipoma, synovium, or accessory muscle). The most common site of compression is the arcade of Frohse (Fig. 6).

US can be used to assess the CSA of the nerve and therefore provide information about the grade of entrapment; however, often only a minor focal swelling or, on the contrary, a long-distance diffuse thickening might be observed.

Dong et al. [41] described the normal CSA values of the posterior interosseus nerve as follows: 1.6 $mm^2$ at 1 cm proximal to the arcade of Frohse and 1.8 $mm^2$ at 1 cm distal to the arcade of Frohse. However, no clear cutoff value has been established for pathologic nerves [42].

Entrapment of the superficial branch of the radial nerve may occur in the distal forearm, leading to a condition known as Wartenberg's syndrome. The causes of nerve entrapment include compression by a bracelet, watch, or handcuff and irritation from an adjacent metal implant after fracture. It may also be associated with de Quervain's tenosynovitis [43]. Symptoms include numbness, tingling, burning, and pain on the back or side of the hand at the base of the thumb. Since the nerve branch is sensory there is no motor impairment.

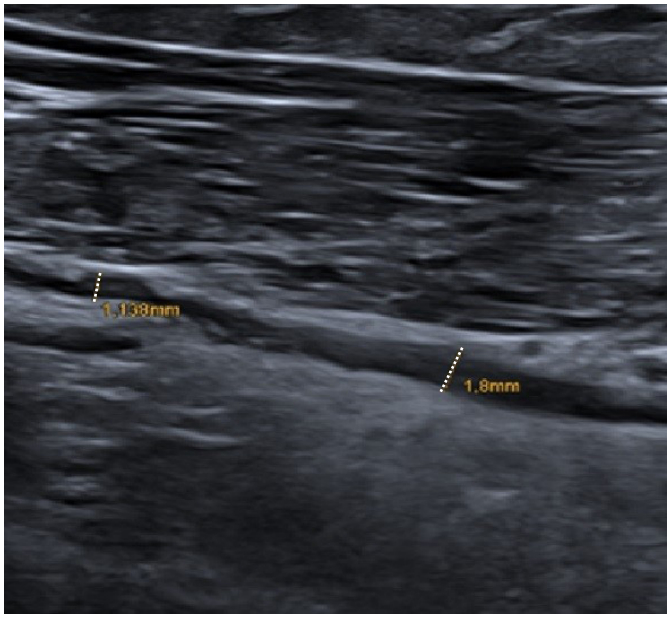


Fig. 6. **A 42-year-old patient presenting with pain at the radial aspect of the cubital fossa.** Ultrasonography shows an irregular hypoechoic radial nerve within the arcade of Frohse.

## Sciatic Nerve/Piriformis Syndrome

Piriformis syndrome is an underdiagnosed entity characterized by pain and/or dysesthesia in the buttock area, hip, or posterior thigh and/or radicular pain due to non-discogenic sciatic nerve entrapment in the subgluteal space [44,45]. Entrapment may occur due to hypertrophy of the muscle or an anomalous course of the sciatic nerve [45,46]. Piriformis syndrome involves a constellation of symptoms that include low back or buttock pain referred to the leg, which is often underdiagnosed and mistaken for more common disorders, including facet arthropathy, sacroiliitis, lumbar disc disease, and radiculopathy [47]. US is a feasible method to measure the thickness of the piriformis muscle, as well as the CSA and course of the sciatic nerve of the pathological site in comparison to the healthy side (Fig. 7) [48].

Wu et al. [49] compared imaging parameters between piriformis syndrome patients and healthy volunteers; both the piriformis thickness and the sciatic nerve diameter on the abnormal side of patients were significantly greater than those of healthy volunteers

(thickness: 21.5 vs. 18.3 mm and diameter: 7.6 vs. 5.9 mm).

## Lateral Femoral Cutaneous Nerve

The lateral femoral cutaneous nerve (LFCN) is a sensory nerve that originates from the lumbar plexus at L2/L3, which is characterized by high anatomic variability, especially at the level of the inguinal ligament and the anterior superior iliac spine [50,51].

Meralgia paresthetica is a disorder related to the entrapment of the LFCN. Patients usually complain of burning pain and/or dysesthesia located at the anterolateral thigh, which may radiate to the knee. Due to the sensory nature of the nerve, there are no changes in any muscles. Obesity, diabetes mellitus, pregnancy, and advancing age are risk factors [51,52].

The course of the LFCN is very superficial; thus, it is susceptible to irritation resulting from causes such as too-tight clothing, especially in obese patients. Moreover, at the site where the LFCN pierces the fascia lata, it may become damaged by a tension mechanism (abrupt hyperextension of the hip) or a compression mechanism (a prolonged standing position). Iatrogenic damage may be caused by a direct anterior approach for total hip arthroplasty. The occurrence of nerve injuries in such procedures is very variable throughout the literature, ranging from 14.8% to 81%; therefore, this represents a frequent and underestimated presentation [48,53].

US findings in positive cases include nerve enlargement (mean, CSA 9 $mm^2$ vs. 3 $mm^2$ in normal controls), nerve hypoechogenicity

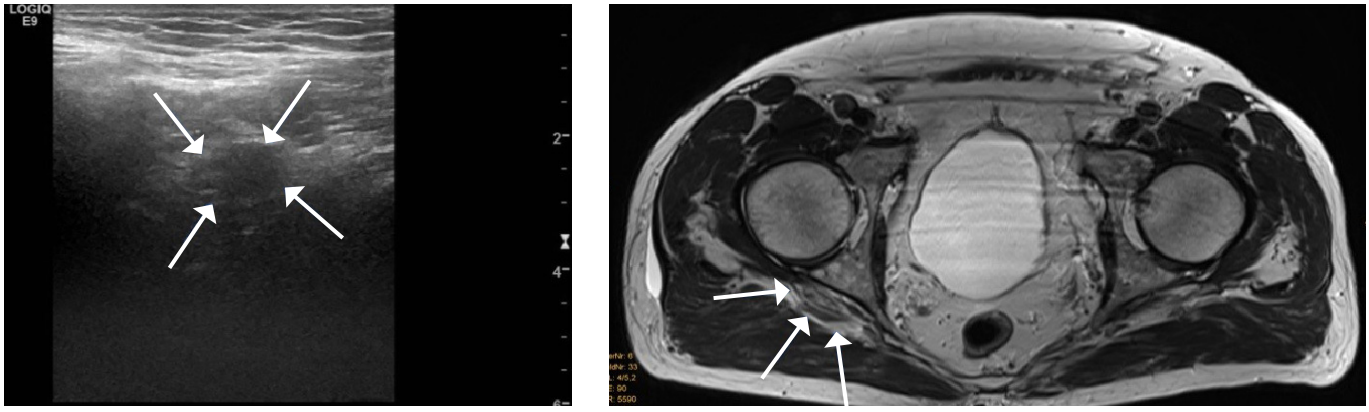

A B

Fig. 7. A 67-year-old patient presenting with sciatica, who underwent previous magnetic resonance imaging of the spine to rule out affection of the nerve roots.
A, B. On ultrasonography (A), the sciatic nerve (arrows) appears hypoechoic and swollen, with corresponding changes of the nerve on T2-weighted magnetic resonance imaging (B).

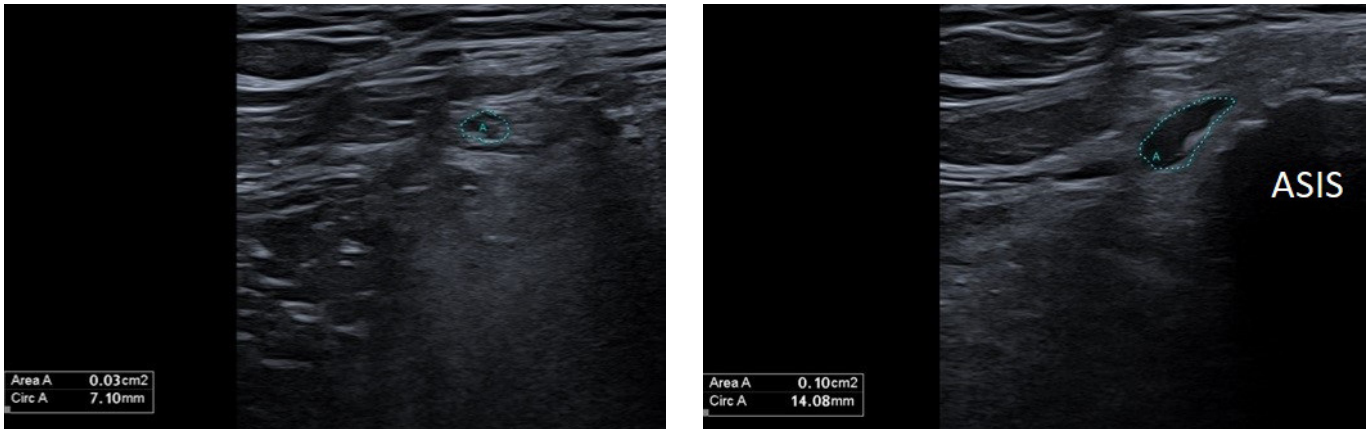


A B

Fig. 8. A 41-year-old patient presenting with numbness and pain in the lateral thigh.
A, B. On ultrasonography, the lateral cutaneous femoris nerve is seen to be hypoechoic and swollen at the level of the anterior superior iliac spine (ASIS) with an increased cross-sectional area.

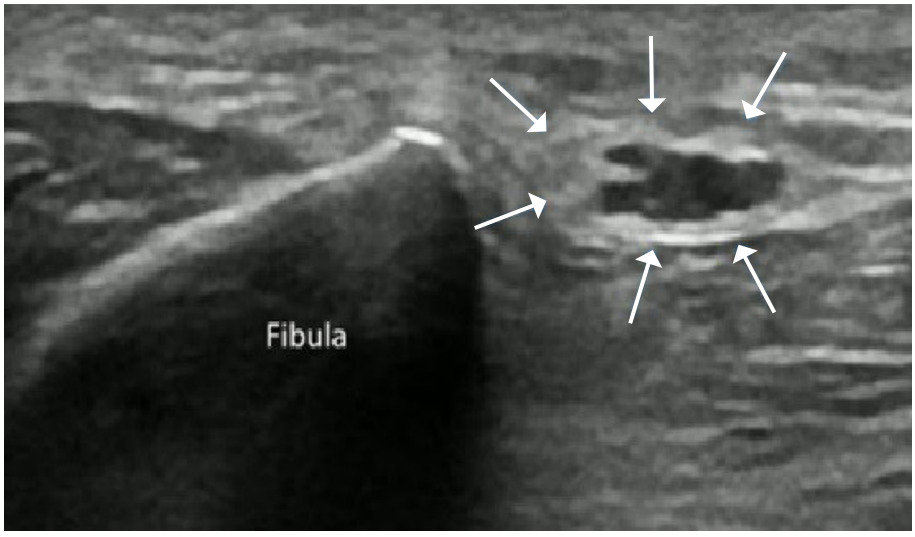


Fig. 9. **A 60-year-old patient presenting with foot drop and numbness in the lower extremity.** On a ultrasonography examination, the common peroneal nerve (arrows) at the level of the fibular head shows swollen fascicles and a thickened perineurium.

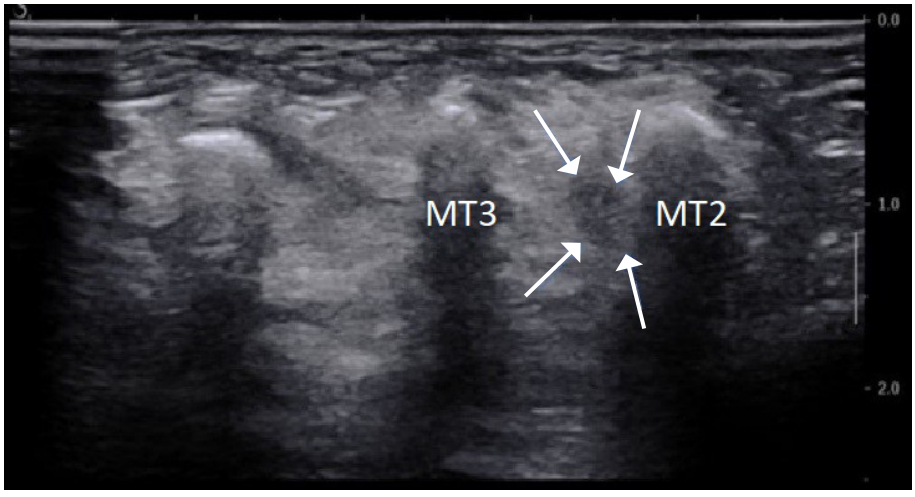


Fig. 10. **A 63-year-old patient with electrifying pain while walking between metatarsal (MT) 2 and 3.** On ultrasonography, a hypoechoic Morton's neuroma (arrows) between the heads of MT 2 and 3 is visible.

in 86%, and focal lesions in 20%, according to a study by Powell et al. [54] (Fig. 8). Interestingly this nerve may be affected not only at the anterior superior iliac spine, but also at different levels along its course, where multiple US-guided injections might be recommended [55].

## Peroneal Nerve

Peroneal neuropathy is the most common compressive neuropathy of the lower extremity. It should be included in the differential diagnosis for patients presenting with foot drop, pain of the lower extremity, or numbness of the lower extremity. Symptoms of peroneal neuropathy may occur due to compression of the common peroneal nerve (CPN), superficial peroneal nerve (SPN), or deep peroneal nerve (DPN), each with different clinical presentations. The CPN is most compressed at the level of the bony prominence of the fibular head, the SPN is most entrapped as it exits the lateral compartment of the leg, and the DPN as it crosses underneath the ankle extensor retinaculum [56–58].

The CPN arises from the sciatic nerve and is subject to a variety of abnormalities. Although the diagnosis is often based on clinical findings and electrodiagnostic tests, high-resolution US plays an increasingly important role in determining the type and location of CPN abnormalities [59].

US can demonstrate an increased CSA of the CPN and changes in nerve echotexture, including the loss of normal fascicular echotexture and an increased echogenic rim (Fig. 9) [60]. The normal mean CSA values at these anatomical sites were reported to be 13.2 $mm^2$ at the fibular head and 11.4 $mm^2$ at the fibular tunnel [61], whereas a CSA of 17.2 $mm^2$ was considered pathological [62].

If the CSA is normal at the fibular head, a further more proximal examination towards the junction with the sciatic nerve should be

performed.

## Morton's Neuroma

According to a study by Quinn et al. [63], US can reveal Morton's neuroma in 85% of cases.

Morton's neuroma is a commonly encountered cause of forefoot pain, which may limit weight-bearing activities and footwear choices. Although the etiology and pathomechanism of this condition remain a matter of debate, the histological endpoint is well established as benign perineural fibrosis of a common plantar digital nerve, typically within the third intermetatarsal space. The most probable cause is a constriction at the level of the intermetatarsal ligament, which in most cases is caused by inappropriate weight put on the forefoot [48,64,65].

A recent study by Del Mar Ruiz-Herrera et al. [66] demonstrated an association between the occurrence of Morton´s neuroma and a smaller space between the metatarsal heads of the third and the fourth metatarsals and under the deep transverse metatarsal ligament using US.

The diagnosis can be accomplished using US with a high level of accuracy and reproducibility [67,68]. The US findings include a reactive tissue mass with a spindle-like shape, presenting with decreased heterogeneous echogenicity and increased vascular flow. Morton's neuroma can be visualized by applying the transducer to the dorsal part of the foot, additionally pressing against the intermetatarsal space from the plantar part. This maneuver enables the movement of the neuroma in the dorsal direction (Fig. 10) [48,69]. Sonographic palpation is further useful when localizing Morton's neuromas, as they can also present variably at a more proximal level and at a dorsal or plantar location. Identification of the presumed plantar digital nerve in continuity with the mass improves diagnostic confidence. The long-axis view often allows the identification of continuity between the common plantar digital nerve and the neuroma. Detection of the plantar digital nerve entering the neuroma can raise the diagnostic accuracy for Morton's neuroma relative to other intermetatarsal masses, such as complicated ganglion cysts or tendon sheath fibromas [70,71].

## Elastography

Although measuring the CSA values of the affected nerves is a good and well-established method, this parameter was also shown to suffer from a lack of standardization, which negatively affected its sensitivity and specificity [72,73]. Sonoelastography is a US imaging technique that allows a noninvasive estimation of tissue stiffness, which might add value to the diagnostic performance of US in entrapment neuropathies [74]. This technique is based on the fact that softer tissue exhibits greater tissue displacement than hard tissue when externally compressed. Entrapment neuropathies are associated with a significant increase in the stiffness of affected nerves, which can be accurately detected with US elastography [72]. Furthermore, Klauser et al. [75] showed that the perineural area, as in CTS, was stiffer in patients than in healthy volunteers.

## Conclusion

High-resolution US is a feasible, fast, and reliable method to diagnose and monitor nerve entrapment syndromes and to guide diagnostic and therapeutic perineural injections. US findings include enlargement of the diameter and CSA of the nerve at the site of compression, hourglass narrowing in the longitudinal section, the loss of echotexture, echogenic perineural fibrosis, decreased mobility, and intraneural fibrosis in longstanding entrapment conditions.

ORCID: Christoph Schwabl: https://orcid.org/0000-0002-4438-9025; Gernot Schmidle: https://orcid.org/0000-0001-7255-799X; Mihra S. Taljanovic: https://orcid.org/0000-0003-1910-6545; Andrea S. Klauser: https://orcid.org/0000-0002-1059-9278

### Author Contributions

Conceptualization: Schwabl C, Schmidle G, Kaiser P, Drakonaki E, Taljanovic MS, Klauser AS. Data acquisition: Schwabl C, Klauser AS. Data analysis or interpretation: Schwabl C, Klauser AS. Drafting of the manuscript: Schwabl C, Klauser AS. Critical revision of the manuscript: Schwabl C, Schmidle G, Kaiser P, Drakonaki E, Taljanovic MS, Klauser AS. Approval of the final version of the manuscript: all authors.

### Conflict of Interest

No potential conflict of interest relevant to this article was reported.

## References

1. Klauser AS, Buzzegoli T, Taljanovic MS, Strobl S, Rauch S, Teh J, et al. Nerve entrapment syndromes at the wrist and elbow by sonography. Semin Musculoskelet Radiol 2018;22:344-353.
2. Menorca RM, Fussell TS, Elfar JC. Nerve physiology: mechanisms of injury and recovery. Hand Clin 2013;29:317-330.
3. Martinoli C, Bianchi S, Pugliese F, Bacigalupo L, Gauglio C, Valle M, et al. Sonography of entrapment neuropathies in the upper limb (wrist excluded). J Clin Ultrasound 2004;32:438-450.
4. Adhikari G, Kayastha P, Suwal S, Paudel S, Chataut D, Maharjan S, et al. Ultrasonographic measurement of mean cross-sectional area of the median nerve in pregnant women in a tertiary level hospital of Nepal: a descriptive cross-sectional study. JNMA J Nepal Med

Assoc 2021;59:180-183.
5. Lee RK, Griffith JF, Ng AW, Tipoe GL, Chan AW, Wong CW, et al. Cross-sectional area of the median nerve at the wrist: comparison of sonographic, MRI, and cadaveric measurements. J Clin Ultrasound 2019;47:122-127.
6. Jenny C, Lutschg J, Broser PJ. Change in cross-sectional area of the median nerve with age in neonates, infants and children analyzed by high-resolution ultrasound imaging. Eur J Paediatr Neurol 2020;29:137-143.
7. Narayan S, Goel A, Singh AK, Thacker AK, Singh N, Gutch M. High resolution ultrasonography of peripheral nerves in diabetic patients to evaluate nerve cross sectional area with clinical profile. Br J Radiol 2021;94:20200173.
8. Pratt E, Vauth H, McIlvain G, Timmons MK. Musicians have thicker median nerve cross sectional area and more symptoms of carpal tunnel than non-musicians. Med Probl Perform Art 2020;35:138-144.
9. Gupta R, Steward O. Chronic nerve compression induces concurrent apoptosis and proliferation of Schwann cells. J Comp Neurol 2003;461:174-186.
10. Gupta R, Rummler LS, Palispis W, Truong L, Chao T, Rowshan K, et al. Local down-regulation of myelin-associated glycoprotein permits axonal sprouting with chronic nerve compression injury. Exp Neurol 2006;200:418-429.
11. Trojaborg W. Rate of recovery in motor and sensory fibres of the radial nerve: clinical and electrophysiological aspects. J Neurol Neurosurg Psychiatry 1970;33:625-638.
12. Doughty CT, Bowley MP. Entrapment neuropathies of the upper extremity. Med Clin North Am 2019;103:357-370.
13. Martinoli C, Bianchi S, Derchi LE. Ultrasonography of peripheral nerves. Semin Ultrasound CT MR 2000;21:205-213.
14. Lawande AD, Warrier SS, Joshi MS. Role of ultrasound in evaluation of peripheral nerves. Indian J Radiol Imaging 2014;24:254-258.
15. Klauser AS, Abd Ellah MM, Halpern EJ, Siedentopf C, Auer T, Eberle G, et al. Sonographic cross-sectional area measurement in carpal tunnel syndrome patients: can delta and ratio calculations predict severity compared to nerve conduction studies? Eur Radiol 2015;25:2419-2427.
16. Chang YW, Hsieh TC, Tzeng IS, Chiu V, Huang PJ, Horng YS. Ratio and difference of the cross-sectional area of median nerve to ulnar nerve in diagnosing carpal tunnel syndrome: a case control study. BMC Med Imaging 2019;19:52.
17. McDonagh C, Alexander M, Kane D. The role of ultrasound in the diagnosis and management of carpal tunnel syndrome: a new paradigm. Rheumatology (Oxford) 2015;54:9-19.
18. Padua L, Padua R, Lo Monaco M, Aprile I, Tonali P. Multiperspective assessment of carpal tunnel syndrome: a multicenter study. Italian CTS Study Group. Neurology 1999;53:1654-1659.
19. Padua L, Coraci D, Erra C, Pazzaglia C, Paolasso I, Loreti C, et al. Carpal tunnel syndrome: clinical features, diagnosis, and management. Lancet Neurol 2016;15:1273-1284.
20. Klauser AS, Faschingbauer R, Bauer T, Wick MC, Gabl M, Arora R, et al. Entrapment neuropathies II: carpal tunnel syndrome. Semin Musculoskelet Radiol 2010;14:487-500.
21. Tagliafico A, Cadoni A, Fisci E, Gennaro S, Molfetta L, Perez MM, et al. Nerves of the hand beyond the carpal tunnel. Semin Musculoskelet Radiol 2012;16:129-136.
22. Smith J, Barnes DE, Barnes KJ, Strakowski JA, Lachman N, Kakar S, et al. Sonographic visualization of thenar motor branch of the median nerve: a cadaveric validation study. PM R 2017;9:159-169.
23. Caetano EB, Vieira LA, Sabongi Neto JJ, Caetano MF, Sabongi RG. Riche-Cannieu anastomosis: structure, function, and clinical significance. Rev Bras Ortop (Sao Paulo) 2019;54:564-571.
24. Sur A, Sinha MM, Ughade JM. Prevalence of Martin-Gruber anastomosis in healthy subjects: an electrophysiological study from Raigarh, Chhattisgarh. Neurol India 2021;69:950-955.
25. Roy J, Henry BM, Pekala PA, Vikse J, Saganiak K, Walocha JA, et al. Median and ulnar nerve anastomoses in the upper limb: a meta-analysis. Muscle Nerve 2016;54:36-47.
26. Rodriguez-Niedenfuhr M, Vazquez T, Parkin I, Logan B, Sanudo JR. Martin-Gruber anastomosis revisited. Clin Anat 2002;15:129-134.
27. Marton A, Ahmed S, Jarvis GE, Brassett C, Grant I, Gaunt ME. The Berrettini palmar neural communicating branch: a study of 27 cadaveric specimens and determination of a high-risk surgical zone. J Hand Surg Eur Vol 2022;47:851-856.
28. Seidel GK, Seidel ME, Hakopian D, Alabdulkarim M, Rahman A, Andary MT, et al. Frequency of electrodiagnostically measurable Berrettini anastomosis. J Clin Neurophysiol 2020;37:214-219.
29. Hobson-Webb LD, Juel VC. Common entrapment neuropathies. Continuum (Minneap Minn) 2017;23:487-511.
30. Beekman R, Visser LH, Verhagen WI. Ultrasonography in ulnar neuropathy at the elbow: a critical review. Muscle Nerve 2011;43:627-635.
31. Plaikner M, Loizides A, Loescher W, Spiss V, Gruber H, Djurdjevic T, et al. Thickened hyperechoic outer epineurium, a sonographic sign suggesting snapping ulnar nerve syndrome? Ultraschall Med 2013;34:58-63.
32. Gruber H, Peer S. The depiction of the cubital segment of the ulnar nerve by high resolution sonography: is it a helpful diagnostic tool for the assessment of the cubital tunnel syndrome? Handchir Mikrochir Plast Chir 2009;41:13-17.
33. Miller TT, Reinus WR. Nerve entrapment syndromes of the elbow, forearm, and wrist. AJR Am J Roentgenol 2010;195:585-594.
34. Sutcliffe J, Ly JQ, Kirby A, Beall DP. Magnetic resonance imaging findings of golf-related injuries. Curr Probl Diagn Radiol 2008;37:231-241.
35. Patterson JM, Jaggars MM, Boyer MI. Ulnar and median nerve palsy in long-distance cyclists: a prospective study. Am J Sports Med

2003;31:585-589.
36. Wick MC, Weiss RJ, Hohlrieder M, Tecklenburg K, Jaschke W, Rieger M. Radiological aspects of injuries of avalanche victims. Injury 2009;40:93-98.
37. Levina Y, Dantuluri PK. Radial tunnel syndrome. Curr Rev Musculoskelet Med 2021;14:205-213.
38. Clavert P, Lutz JC, Adam P, Wolfram-Gabel R, Liverneaux P, Kahn JL. Frohse's arcade is not the exclusive compression site of the radial nerve in its tunnel. Orthop Traumatol Surg Res 2009;95:114-118.
39. Strohl AB, Zelouf DS. Ulnar tunnel syndrome, radial tunnel syndrome, anterior interosseous nerve syndrome, and pronator syndrome. J Am Acad Orthop Surg 2017;25:e1-e10.
40. Sarris IK, Papadimitriou NG, Sotereanos DG. Radial tunnel syndrome. Tech Hand Up Extrem Surg 2002;6:209-212.
41. Dong Q, Jamadar DA, Robertson BL, Jacobson JA, Caoili EM, Gest T, et al. Posterior interosseous nerve of the elbow: normal appearances simulating entrapment. J Ultrasound Med 2010;29:691-696.
42. Becciolini M, Pivec C, Raspanti A, Riegler G. Ultrasound of the radial nerve: a pictorial review. J Ultrasound Med 2021;40:2751-2771.
43. Chang KV, Mezian K, Nanka O, Wu WT, Lou YM, Wang JC, et al. Ultrasound imaging for the cutaneous nerves of the extremities and relevant entrapment syndromes: from anatomy to clinical implications. J Clin Med 2018;7:457.
44. Hernando MF, Cerezal L, Perez-Carro L, Abascal F, Canga A. Deep gluteal syndrome: anatomy, imaging, and management of sciatic nerve entrapments in the subgluteal space. Skeletal Radiol 2015;44:919-934.
45. Carro LP, Hernando MF, Cerezal L, Navarro IS, Fernandez AA, Castillo AO. Deep gluteal space problems: piriformis syndrome, ischiofemoral impingement and sciatic nerve release. Muscles Ligaments Tendons J 2016;6:384-396.
46. Marco C, Miguel-Perez M, Perez-Bellmunt A, Ortiz-Sagrista JC, Martinoli C, Moller I, et al. Anatomical causes of compression of the sciatic nerve in the pelvis: piriform syndrome. Rev Esp Cir Ortop Traumatol (Engl Ed) 2019;63:424-430.
47. Tagliafico A, Bodner G, Rosenberg I, Palmieri F, Garello I, Altafini L, et al. Peripheral nerves: ultrasound-guided interventional procedures. Semin Musculoskelet Radiol 2010;14:559-566.
48. Kowalska B, Sudol-Szopinska I. Ultrasound assessment of selected peripheral nerves pathologies. Part II: Entrapment neuropathies of the lower limb. J Ultrason 2012;12:463-471.
49. Wu YY, Guo XY, Chen K, He FD, Quan JR. Feasibility and reliability of an ultrasound examination to diagnose piriformis syndrome. World Neurosurg 2020;134:e1085-e1092.
50. Carai A, Fenu G, Sechi E, Crotti FM, Montella A. Anatomical variability of the lateral femoral cutaneous nerve: findings from a surgical series. Clin Anat 2009;22:365-370.
51. Becciolini M, Pivec C, Riegler G. Ultrasound of the lateral femoral cutaneous nerve: a review of the literature and pictorial essay. J Ultrasound Med 2022;41:1273-1284.
52. Parisi TJ, Mandrekar J, Dyck PJ, Klein CJ. Meralgia paresthetica: relation to obesity, advanced age, and diabetes mellitus. Neurology 2011;77:1538-1542.
53. Dahm F, Aichmair A, Dominkus M, Hofstaetter JG. Incidence of lateral femoral cutaneous nerve lesions after direct anterior approach primary total hip arthroplasty: a literature review. Orthop Traumatol Surg Res 2021;107:102956.
54. Powell GM, Baffour FI, Erie AJ, Puffer RC, Spinner RJ, Glazebrook KN. Sonographic evaluation of the lateral femoral cutaneous nerve in meralgia paresthetica. Skeletal Radiol 2020;49:1135-1140.
55. Klauser AS, Abd Ellah MM, Halpern EJ, Sporer I, Martinoli C, Tagliafico A, et al. Meralgia paraesthetica: Ultrasound-guided injection at multiple levels with 12-month follow-up. Eur Radiol 2016;26:764-770.
56. Fortier LM, Markel M, Thomas BG, Sherman WF, Thomas BH, Kaye AD. An update on peroneal nerve entrapment and neuropathy. Orthop Rev (Pavia) 2021;13:24937.
57. Canella C, Demondion X, Guillin R, Boutry N, Peltier J, Cotten A. Anatomic study of the superficial peroneal nerve using sonography. AJR Am J Roentgenol 2009;193:174-179.
58. Nwawka OK, Lee S, Miller TT. Sonographic evaluation of superficial peroneal nerve abnormalities. AJR Am J Roentgenol 2018;211:872-879.
59. Grant TH, Omar IM, Dumanian GA, Pomeranz CB, Lewis VA. Sonographic evaluation of common peroneal neuropathy in patients with foot drop. J Ultrasound Med 2015;34:705-711.
60. Bignotti B, Assini A, Signori A, Martinoli C, Tagliafico A. Ultrasound versus MRI in common fibular neuropathy. Muscle Nerve 2017;55:849-857.
61. Tagliafico A, Cadoni A, Fisci E, Bignotti B, Padua L, Martinoli C. Reliability of side-to-side ultrasound cross-sectional area measurements of lower extremity nerves in healthy subjects. Muscle Nerve 2012;46:717-722.
62. Bignotti B, Cadoni A, Assini A, Martinoli C, Tagliafico A. Fascicular involvement in common fibular neuropathy: evaluation with ultrasound. Muscle Nerve 2016;53:532-537.
63. Quinn TJ, Jacobson JA, Craig JG, van Holsbeeck MT. Sonography of Morton's neuromas. AJR Am J Roentgenol 2000;174:1723-1728.
64. Mak MS, Chowdhury R, Johnson R. Morton's neuroma: review of anatomy, pathomechanism, and imaging. Clin Radiol 2021;76:235.
65. Jain S, Mannan K. The diagnosis and management of Morton's neuroma: a literature review. Foot Ankle Spec 2013;6:307-317.
66. Del Mar Ruiz-Herrera M, Criado-Alvarez JJ, Suarez-Ortiz M, Konschake M, Moroni S, Marcos-Tejedor F. Study of the anatomical association between Morton's neuroma and the space inferior to the deep transverse metatarsal ligament using ultrasound. Diagnostics (Basel) 2022;12:1367.

67. Xu Z, Duan X, Yu X, Wang H, Dong X, Xiang Z. The accuracy of ultrasonography and magnetic resonance imaging for the diagnosis of Morton's neuroma: a systematic review. Clin Radiol 2015;70:351-358.
68. Park YH, Choi WS, Choi GW, Kim HJ. Intra- and interobserver reliability of size measurement of Morton neuromas on sonography. J Ultrasound Med 2019;38:2341-2345.
69. De Maeseneer M, Madani H, Lenchik L, Kalume Brigido M, Shahabpour M, Marcelis S, et al. Normal anatomy and compression areas of nerves of the foot and ankle: US and MR imaging with anatomic correlation. Radiographics 2015;35:1469-1482.
70. Son HM, Chai JW, Kim YH, Kim DH, Kim HJ, Seo J, et al. A problem-based approach in musculoskeletal ultrasonography: central metatarsalgia. Ultrasonography 2022;41:225-242.
71. Gimber LH, Melville DM, Bocian DA, Krupinski EA, Guidice MP, Taljanovic MS. Ultrasound evaluation of Morton neuroma before and after laser therapy. AJR Am J Roentgenol 2017;208:380-385.
72. Dabrowska-Thing A, Zakrzewski J, Nowak O, Nitek Z. Ultrasound elastography as a potential method to evaluate entrapment neuropathies in elite athletes: a mini-review. Pol J Radiol 2019;84:e625-e629.
73. Pastare D, Therimadasamy AK, Lee E, Wilder-Smith EP. Sonography versus nerve conduction studies in patients referred with a clinical diagnosis of carpal tunnel syndrome. J Clin Ultrasound 2009;37:389-393.
74. Hall TJ. AAPM/RSNA physics tutorial for residents: topics in US: beyond the basics: elasticity imaging with US. Radiographics 2003;23:1657-1671.
75. Klauser AS, Miyamoto H, Martinoli C, Tagliafico AS, Szantkay J, Feuchtner G, et al. Sonoelastographic findings of carpal tunnel injection. Ultraschall Med 2015;36:618-622.